

Numerical Prediction of Contact Line Dynamics on Super-Hydrophobic Surfaces

Ashwin Ramesh, S.V. Diwakar and Sarit K. Das*

Department of Mechanical Engineering,
Indian Institute of Technology Madras,
Chennai - 600036, India

ABSTRACT

The current study numerically investigates the motion of droplets on a surface with a micro cavity using the Volume of Fluid (VOF) technique. The simulation is a precursor to droplet motion on super-hydrophobic surfaces which is the focus of surface engineering research in recent times. The advancing and receding contact angles are tracked as a droplet moves on a single cavity which can be seen as the space between two posts of a typical engineered super-hydrophobic surface. Stick-jump-slip behavior can be seen during the advancing motion of the drop and the reverse is seen during the receding motion. The contact angle evolution is studied for three different post geometries and it is concluded that wider post spacing leads to smaller dynamic contact angles. This study is important from the point of prediction of dynamic contact angles computationally on super-hydrophobic surfaces.

Keywords: *Super-hydrophobic surface, dynamic contact angle, droplet motion, VOF method*

1. INTRODUCTION

Super-hydrophobic surfaces are surfaces with contact angle (between the drop and the surface) greater than 150° . Such surfaces are also called non-wettable surfaces. Research in super-hydrophobic effect is inspired by the so called "Lotus Effect". The lotus leaf exhibits such super-hydrophobicity due to the presence of posts of the order of a few microns on its surface. The phenomenon was first studied by Johnson and Dettre in 1964 [1] using rough hydrophobic surfaces made of glass beads coated with paraffin or PTFE polymer. Super-hydrophobic surfaces also exhibit what is called the self cleaning property [1]. Due to this property, such surfaces have important real-life applications. They are used as lacquers for vehicles, water-proof clothes and textiles, windshields and window glasses, etc. [2, 3].

Understanding drop dynamics on super-hydrophobic surfaces is important from the applications standpoint of these surfaces. Droplets tend to minimize their surface energy and thus the surface area and try to achieve a spherical shape. On contact with a surface, adhesion forces try to disrupt this and result in spreading of the droplet on the surface. Complete or incomplete wetting may occur depending on the nature of the surface and the surface tension of the droplet. In order to minimize the adhesion forces and introduce super-hydrophobicity, surfaces have to be engineered in such a way that they have a low surface energy. This low surface energy can be achieved through a variety of ways like micro-texturing, water repellent coatings, nano-wires, etc. [4–7].

The hydrophobicity of a surface is determined by the contact angle. Surfaces with a contact angle less than 90° are referred to as hydrophilic and those with an angle greater than 90° as hydrophobic. Some surfaces show contact angles up to 150° and are called super-hydrophobic surfaces. Thus, higher

*Corresponding author. Email: skdas@iitm.ac.in

contact angles are preferred for water repellency and self-cleaning properties. Droplets on a super-hydrophobic surface can be in two states, the Cassie state or suspended state, where the drop sits on top of the posts with pockets of air beneath it, or Wenzel state or collapsed state, where the drop fills the gaps between the posts. Several authors have calculated the free energies of the Cassie and Wenzel states using approximations based on the Cassie-Baxter and Wenzel laws [8, 9] respectively. The stability of each of these states depends on the initial conditions and the nature of the droplet and the surface. The suspended drop is often observed to be in a meta-stable state as it has to cross a free energy barrier to fill the grooves. However, the kinetics of transition to the collapsed phase is not understood and it is hard to probe experimentally. The reason why this appeals to microchannels researchers is that a water drop on a hydrophobic surface rolls off much easily (or at a much lower surface gradient) as compared to hydrophilic surfaces. This is because of the decreased contact surface area that results in reduced friction. Applied to microchannels, this would result in lower pressure drop across the channel, reducing one major drawback of these channels in practical applications.

When a drop is in motion (moving contact line), the contact angle of the drop deviates from its equilibrium value depending on various factors like surface topology, velocity of drop, etc. This deviated contact angle, while the drop is in motion, is called dynamic contact angle. The drop assumes a distorted shape and the front part of the drop has a contact angle higher than the equilibrium contact angle while the receding part has a lower one. These two are referred to as advancing and receding contact angles respectively. The advancing contact angle is defined as the maximum angle attained by a drop when liquid is added to it, provided the contact line is fixed. Similarly, the receding contact angle is defined as the minimum angle attained by the drop when liquid is removed from it, provided the contact line is fixed. The difference between the advancing and the receding angle is referred to as the Contact Angle Hysteresis (CAH).

A large number of studies on super-hydrophobic surfaces have come out for both static and dynamic conditions which are primarily experimental in nature [10–14]. Although they have brought out valuable information, they are seriously limited by experimental hardware, particularly for droplet dynamics. Thus, a need for developing proper strategy for numerical simulation of flow over super hydrophobic surfaces has been strongly felt.

The earliest numerical simulations of superhydrophobic behavior were performed on a single droplet of fluid perched atop a series of rectangular posts. Dupuis and Yeomans (2005) [15] presented a free energy lattice Boltzmann solution of the spreading of droplets on topologically patterned substrates. Dupuis and Yeomans (2006) [16] also presented a lattice Boltzmann solution to the equations of motion describing the movement of droplets on topologically patterned substrates. It was done to model superhydrophobic behavior on surfaces covered by an array of micron-scale posts. It was found that the posts resulted in a substantial increase in contact angle, from 110° to 156° . Similarly, Zhang et al. [17] investigated the contact line motion of a droplet on a super-hydrophobic surface using the Lattice Boltzmann technique and predicted what is called the stick-jump-slip motion on a super-hydrophobic surface. Although, there has been significant amount of study on the drop motion on super-hydrophobic surfaces using the Lattice Boltzmann technique, it goes without saying that such stochastic computational techniques are computationally intensive and expensive. It is difficult to use such techniques for larger and complex computational domains. On the other hand rapidly developing interface tracking techniques such as the Volume of Fluid (VOF) method offers an excellent alternative by virtue of being computationally efficient and inexpensive. However, challenges such as incorporating surface tension forces effectively to the continuum formulation, grid resolution near boundary and temporal resolution for capture of hysteresis are formidable for which such approaches has been lacking in literature. The current study tries to bridge this gap and aims at presenting a strategy for predicting the advancing and receding contact angles as well as the stick-jump-slip phenomenon on a super-hydrophobic surface modeled by a single micro cavity.

2. MATHEMATICAL MODEL

The contact angle is tracked as a droplet moves over a super-hydrophobic 2-D surface. The surface is characterized by the presence of a single micro-post with width varying between 25 and 75 μm (Fig 1). The height of the micro-post is fixed at 50 μm . The domain is a rectangular geometry with dimensions 1 mm \times 2 mm and the drop diameter is 0.5 mm.

2.1. Model for interface tracking

The volume of fluid model tracks the content of each phase in the computational cell by using the volume fraction, defined as the ratio of volume of one phase to the total volume of the cell.

$$\alpha_q = 0, \text{ The cell is empty of phase } q$$

$$\alpha_q = 1, \text{ The cell is full of phase } q$$

$$0 < \alpha_q < 1, \text{ The cell has an interface involving phase } q$$

The mass conservation necessitates that the summation of all the phase content variables is equal to one in a given cell.

$$\sum_{q=1}^n \alpha_q = 1, \text{ for all phases}$$

The additional tracking of phase information requires the solution of a saturation transport equation in addition to the set of regular fluid dynamics equations:

$$\frac{\partial \alpha_q}{\partial t} + V \cdot \nabla \alpha_q = 0$$

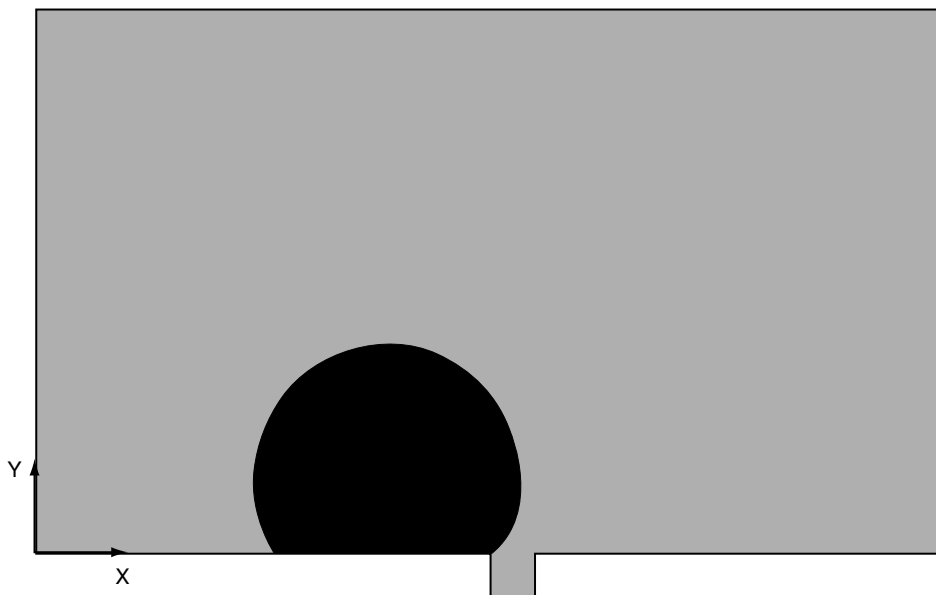


Figure 1. Sketch of the problem considered.

The equation is discretized using an explicit Euler scheme. The volume fraction at the current time step is calculated explicitly using the data from the previous time step, making the method non-iterative.

$$\frac{\alpha_q^{n+1} - \alpha_q^n}{\Delta t} + \frac{\Delta(U_f^n \alpha_{qf}^n)}{V} = 0$$

n = the previous time step

$n + 1$ = the current time step

α_{qf} = face value of volume fraction

V = volume of cell

U_f = Volume flux through face f

Any property (B) of the fluid mixture in a cell is obtained as a weighted average of the properties of the individual components. The weighting function used here directly corresponds to the volume fraction of the component in the cell.

$$B = \sum_{q=1}^n \alpha_q B_q$$

These averaged properties are used in a single momentum equation in order to solve the flow velocity field.

$$\frac{\partial}{\partial t} \rho u_j + \frac{\partial}{\partial x_i} \rho u_i u_j = - \frac{\partial p}{\partial x_j} + \frac{\partial}{\partial x_i} \mu \left(\frac{\partial u_i}{\partial x_j} + \frac{\partial u_j}{\partial x_i} \right) + \rho g_j + F_j$$

The interface in the VOF method is reconstructed based upon the volume fraction of the phases in surrounding cells. The reconstruction process uses a piecewise linear approximation (PLIC) of the phase boundaries.

2.2. Modeling of surface tension

Surface tension is modeled using the continuum surface force model (Brackbill et al. [18]), which is based on a pressure jump across the interface boundary.

$$\Delta P_{1-2} = \sigma \left(\frac{1}{R_2} + \frac{1}{R_1} \right)$$

R_1 and R_2 are the radius of curvature of the interface along the two orthogonal slice planes. In this method the surface force due to interfacial tension is converted to a volume force over a thin layer around the interface. The curvature values are obtained by using a mollified (smoothened) volume fraction data instead of the actual discrete volume fractions. The surface normal is calculated as the gradient of the mollified volume fraction of primary phase.

$$n = \nabla \tilde{\alpha}_1$$

The curvature of the interface is then given by the divergence of the interface unit normal as

$$\kappa = \nabla \cdot \hat{n} = \left[\left(\frac{n}{|n|} \cdot \nabla \right) - \frac{1}{|n|} (\nabla \cdot n) \right]$$

Using these interfacial curvature values, the volumetric approximation of surface tension force is given as,

$$F_{vol} = 2\sigma\kappa\alpha_1\nabla\alpha_1$$

2.3. Numerical technique and grid independence

A commercial CFD software FLUENT is used to track the interface of the droplet and apply the finite volume discretizations of the above mathematical formulations. Pressure is discretized using the pressure staggering method (often abbreviated as PRESTO) and pressure and velocity are decoupled using the SIMPLE (Semi-Implicit Method for Pressure Linked Equations) algorithm. A convergence criterion of 10^{-5} is set for all the equations like continuity, momentum, etc.

The computational domain is shown in figure 1 with a drop of 0.5 mm diameter placed on a wall with a single post. No slip boundary condition is applied at the walls where the drop is in contact. A horizontal acceleration is applied to the drop to enable its horizontal direction motion. Outflow boundary conditions are fixed at the remaining three boundaries of the computational domain (Fig 2). A contact angle of 120° was set between the drop and the wall when the drop was completely in contact with the bottom surface. The contact angle evolution as the drop slides over the column of air trapped is obtained from the solution.

Figure 2 shows the typical grid used for the computational domain along with the appropriate boundary conditions. This particular grid is of size $5\ \mu\text{m}$.

Grid Independence study is performed to ensure that the properties of the grid do not affect the final solution. This is typically done by obtaining a solution for four different grid sizes and comparing the difference in the solution. Table 1 shows the evolution of the advancing contact angle with time for four different grid sizes – 2, 2.5, 5 and 10 microns. It can be seen from Fig. 3 that 2 micron grid size and 2.5 micron grid size have similar contact angle characteristics and hence all the simulations are performed with 2.5 micron grid spacing.

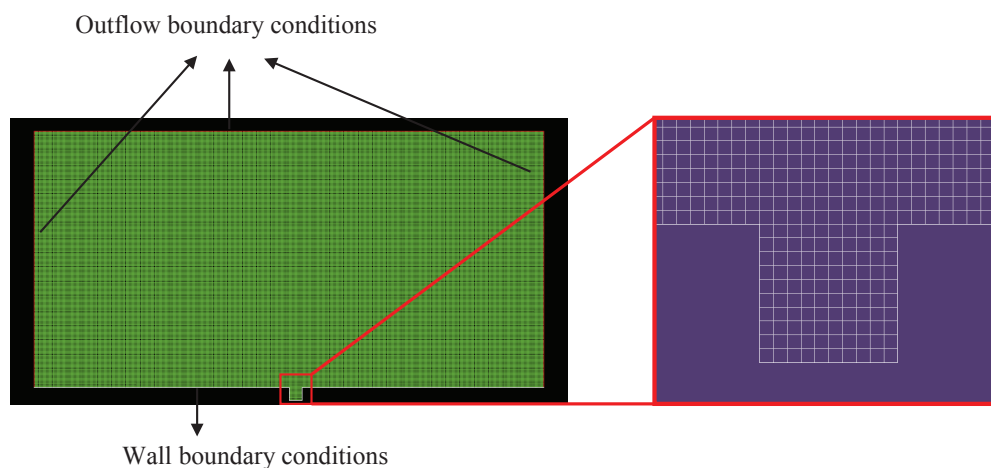


Figure 2. Simulation cell with boundary conditions and grid formulation.

Table 1. Contact angle variation for four grid sizes.

10 microns		5 microns		2.5 microns		2 microns	
Time (s) ($\times 10^4$)	Contact angle ($^\circ$)	Time (s) ($\times 10^4$)	Contact angle ($^\circ$)	Time (s) ($\times 10^4$)	Contact angle ($^\circ$)	Time (s) ($\times 10^4$)	Contact angle ($^\circ$)
1.54	124	1.75	136	1.87	138	1.96	139
1.69	133	2.21	147	2.34	152	2.44	152
1.86	141	2.64	155	2.75	157	2.84	157
2.07	145	3.02	159	3.12	159	3.22	160
2.28	148	3.34	164	3.46	163	3.55	164
2.49	151	3.71	165	3.79	167	3.88	168
2.69	154	4.04	169	4.08	171	4.17	171
2.88	157	4.33	173	4.34	175	4.44	176

Table 2. Advancing contact angle as a function of time for three different post geometries.

25 μm		50 μm		75 μm	
Time (s) ($\times 10^4$)	Contact angle ($^\circ$)	Time (s) ($\times 10^4$)	Contact angle ($^\circ$)	Time (s) ($\times 10^4$)	Contact angle ($^\circ$)
1.55	126	1.87	138	1.55	139
1.74	142	2.34	152	2.10	140
2.11	153	2.75	157	2.70	152
2.73	163	3.46	163	3.27	158
3.27	165	3.79	167	3.77	166
4.18	177	4.08	171	4.19	172
4.72	179	4.60	179	4.95	180

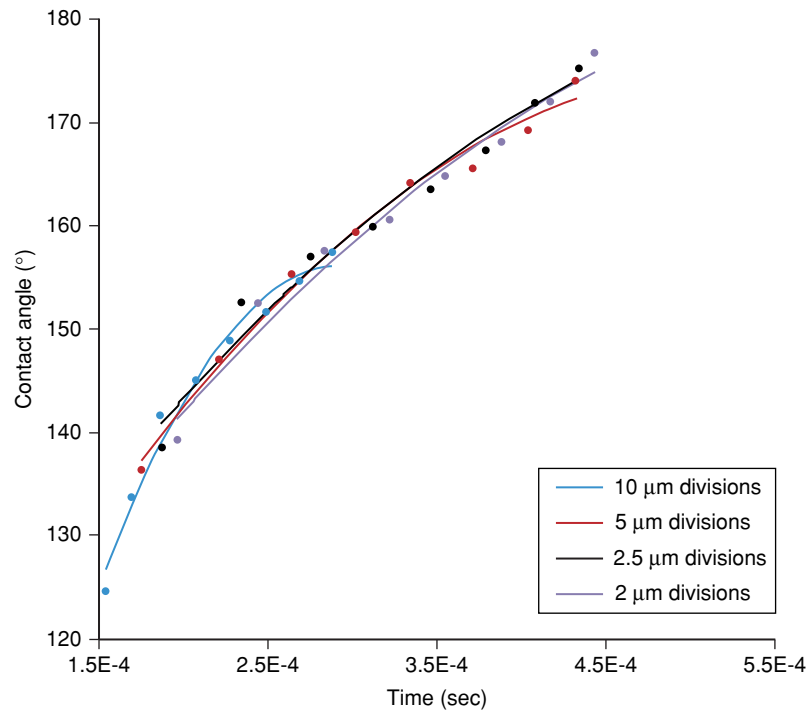


Figure 3. Plot of Contact angle variation vs time for four different grid sizes.

3. RESULTS AND DISCUSSION

The overall formulation described above is used to simulate the movement of the droplet over the chosen geometry. Snapshots of the advancing liquid – vapor interface during the period are provided in Fig. 4i (a-f). It can be seen that, because of the hydrophobic nature of the surface, the Laplace pressure prevents the liquid from penetrating into the gaps, and thus, vapor is trapped. This is the most important character of super-hydrophobic surfaces and this simulation captured it well. The other aspect of flow of droplet over superhydrophobic surface is the pinning of the contact line at the leading edge of the droplet. The consequence of this is the gradual increase or decrease of the contact angle as the drop advances over the air gap. The figure clearly demonstrates that this feature of the droplet motion is perfectly captured by the present simulation. These results also highlight the super-hydrophobic characteristic of trapped air in the micro-void. The receding phase of the drop is a reverse of the advancing phase (Fig. 4ii (a-d)). This phenomenon can be called jump-stick-slip behavior. The figure highlights this behavior as the drop initially jumps to the right post and then pins to the right until it attains the receding contact angle followed by slipping over the surface. The phenomenon of stick-jump-slip is captured accurately during the advancing phase of the droplet.

Here, the advancing and receding contact angle evolution has been numerically predicted through the VOF model. Fig 4 highlights that as the pinning takes place at the left side of the post and the contact angle increases until the drop touches the right side of the post, the subsequent motion of the trailing edge of the droplet is also replicated accurately. The most challenging of them is the simulation of the trailing edge to bring its jump over the cavity and the present simulation performs that perfectly. In this case, the drop “jumps” across the micro-post and gets pinned to the right side of the post. Thereafter, the contact angle changes to the dynamic receding value and the drop continues moving.

Fig 5 shows the evolution of the liquid-air interface as predicted by Zhang et al. [17] using the Lattice Boltzmann Technique (LBM). The VOF simulations show similar trends compared to the LBM approach. However, Zhang et al. [17] showed the evolution of contact angle on a super-hydrophobic surface using the computationally intensive Lattice Boltzmann Technique. Whereas, in this, study we predict the evolution using the VOF method using computational technique of continuum fluid mechanics with much simpler effort.

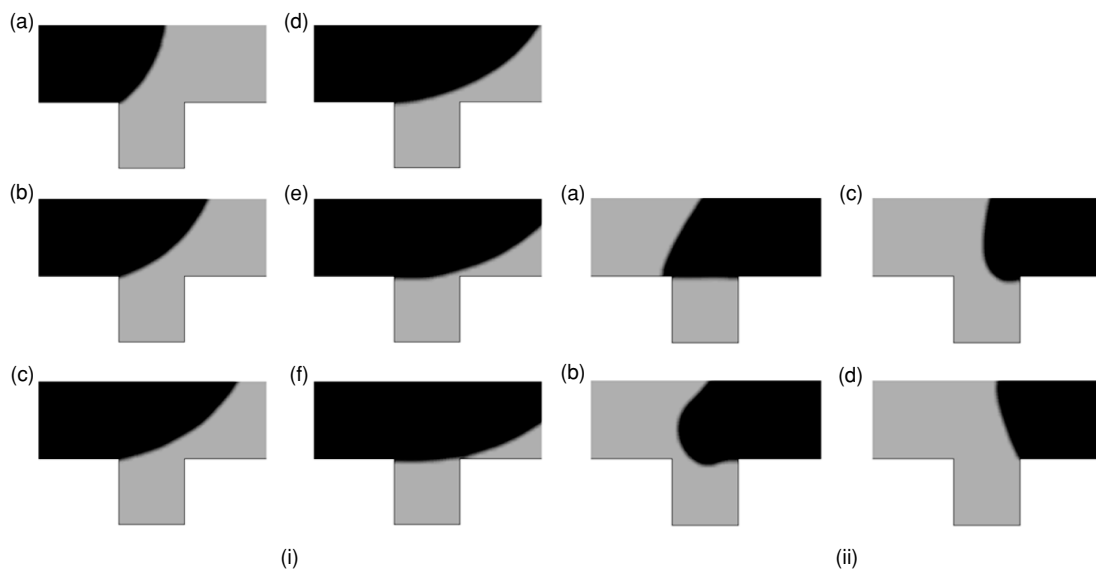


Figure 4. Droplet pinning on edge of the micro-post. Figure to the left (i) shows the evolution of the advancing contact angle and figure to the right (ii) shows the receding contact angle. The direction of motion of the drop is towards the right (positive x-axis).

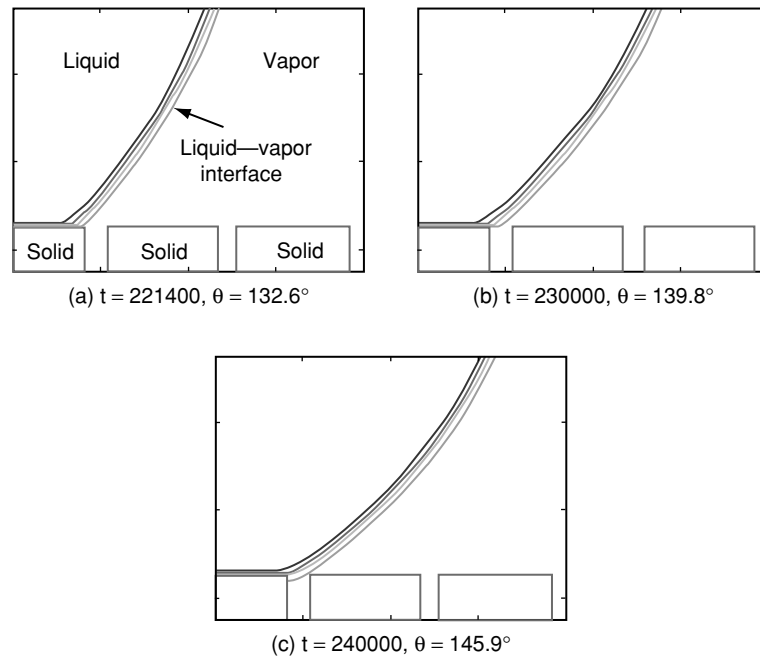


Figure 5. Droplet pinning as predicted by Zhang et al. (2006).

Three different post geometries were considered for the parametric study. Post widths of 25 μm , 50 μm and 75 μm with a contact post height of 50 μm were studied and the contact angle evolution with time for these post geometries is shown in figure 6. Like Fig 4 these simulations also highlight the

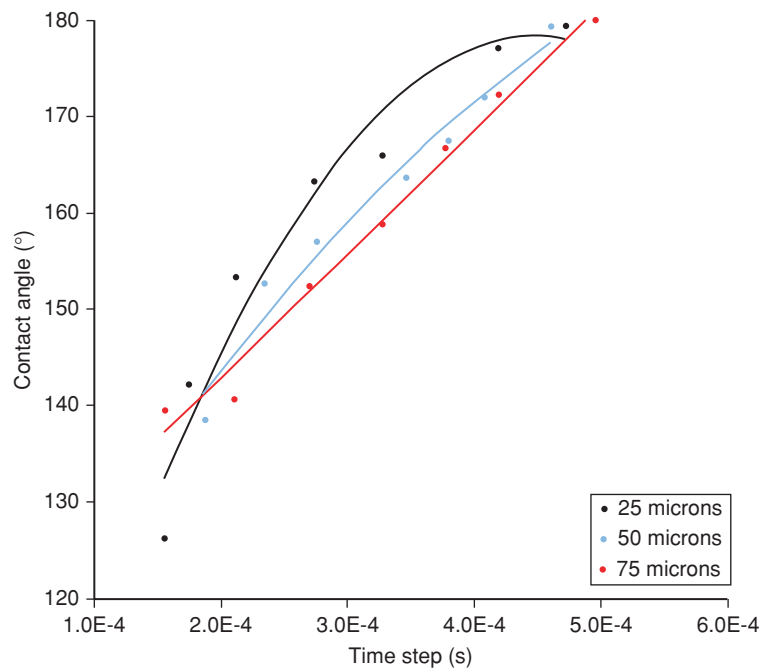


Figure 6. Plot of contact angle vs time for three post geometries.

advancing and receding contact angle evolution with time for a drop moving over a single hydrophobic post. The parametric study performed indicates the dependence of contact angle on the post geometry. From figure 6, it can be seen that a wider post results in a smaller dynamic contact angle and hence, increased drag.

4. CONCLUSIONS

There is widespread confusion whether conventional fluid dynamic techniques can be used to accurately capture the microscale flow problems. The situation is even more complex when at such scales, multiple phases are involved. Distinctive features such as dynamic contact angle and its hysteresis, contact line movement and pinning, stick-jump-slip phenomenon have been addressed with non continuum approach like Lattice-Boltzmann technique. This study shows that the classical continuum approach with interface tracking algorithm such as Volume of Fluid method can be used to accurately predict the characteristics of drop motion over super-hydrophobic surfaces. The pinning of contact line, variation of local contact angle and stick-jump-slip behavior during the advancing and the receding phases were captured accurately using this model. Understanding the dynamic wetting behavior is important while designing super-hydrophobic surfaces. It has to be noted that super-hydrophobic surfaces must not be designed based on static contact angles alone and the dynamic behavior also has to be taken into account especially in applications which involve droplet sliding. In realizing such designs, the present simple method can play a significant role.

REFERENCES

- [1] Johnson Jr. Rulon E., Robert H. Dettre, 1964, Contact Angle Hysteresis. III. Study of an Idealized Heterogeneous Surface, *J. Phys. Chem.*, 68(7), pp. 1744–1750.
- [2] Baumann, M, G, Sakoske, L, Poth, G, Tünker., 2003. Learning from the lotus flower – selfcleaning coatings on glass. *Proceedings of the 8th international glass conference*, pp. 330–333.
- [3] Pociute, M, B, Lehmann, A, Vitkauskas, 2003. Wetting behavior of surgical polyester woven fabrics. *Mater. Sci.*, 9, 410–413.
- [4] Höcker, H, 2002. Plasma treatment of textile fibres, *Pure Appl. Chem.*, 74, 423–427.
- [5] Chien-Te Hsieh, Fang-Lin Wu, Shu-Ying Yang, 2008. Superhydrophobicity from composite nano/microstructures: Carbon fabrics coated with silica nanoparticles. *Surface & Coatings Technology*, 202: 6103–6108.
- [6] Taolei Sun, Lin Feng, Xuefeng Gao, Lei Jiang, 2005. Bioinspired Surfaces with Special Wettability. *Acc. Chem. Res.*, 38(8), pp. 644–652.
- [7] Ning Zhao, Jian Xu, Qiongdan Xie, Lihui Weng, Xinglin Guo, Xiaoli Zhang, Lianghe Shi, 2005. Fabrication of Biomimetic Superhydrophobic Coating with a Micro-Nano-Binary Structure. *Macromolecular Rapid Communications* 26: 1075–1080.
- [8] Cassie, ABD; Baxter, S; 1944. Wettability of Porous Surfaces. *Trans. Faraday Soc.* 40: 546–551.
- [9] Wenzel, RN. 1936. Resistance of Solid Surfaces to Wetting by Water. *Ind. Eng. Chem.* 28: 988–994.
- [10] Choi, Wonjae, Anish Tuteja, Joseph M, Mabry, Robert E, Cohen, Gareth H, McKinley, 2009. A Modified Cassie-Baxter Relationship to Explain Contact Angle Hysteresis and Anisotropy on Non-Wetting Textured Surfaces. *Journal of Colloids and Interfacial Science* 339, 208–216.
- [11] Vaibhav Bahadur, Suresh V, Garimella, 2007. Electrowetting based control of static droplet states on rough surfaces, *Langmuir*, 23(9), 4918–4924.
- [12] Tom N. Krupenkin, J, Ashley Taylor, Evelyn N, Wang, Paul Kolodner, Marc Hodes, Todd R, Salamon, 2007. Reversible Wetting-Dewetting Transitions on Electrically Tunable Superhydrophobic Nanostructured Surfaces, *Langmuir*, 23(18), 9128–9133.

- [13] Anish Tuteja, Wonjae Choi, Gareth H, McKinley, Robert E, Cohen, Michael F, Rubne, 2008. Design parameters for superhydrophobicity and superoleophobicity. *MRS Bulletin*, Vol. 33, 752–758.
- [14] Varanasi, K, K, Tao Deng, Ming F, Hsu, Nitin Bhate, 2009. Wetting Hysteresis, Metastability, and Droplet Impact on Superhydrophobic Surfaces; *Proceedings of IPACK2009*.
- [15] A. Dupuis, J, M, Yeomans, 2005. Modeling Droplets on Superhydrophobic Surfaces: Equilibrium States and Transitions, *Langmuir*, 21, 2624–2629.
- [16] A. Dupuis, J, M, Yeomans, 2006. Dynamics of sliding drops on superhydrophobic surfaces, *Europhys. Lett.* 75 105.
- [17] Junfeng Zhang, Daniel Y, Kwok, 2006. Contact Line and Contact Angle Dynamics in Superhydrophobic Channels. *Langmuir* 22(11), pp. 4998–5004.
- [18] Brackbill, J.U, Kothe D, B, Zemach C, 1992. A continuum method for modeling surface tension. *J. Comput. Phys.* 100, 335–354.